Article

Mechanical Properties of NiTi Rotary Files Fabricated through Gold-Wire, CM-Wire, T-Wire, and R-Phase Heat Treatment

Soram Oh [1], Tae-Hwan Kim [2] and Seok Woo Chang [1,*]

1   Department of Conservative Dentistry, College of Dentistry, Kyung Hee University Medical Center, Kyung Hee University, 23 Kyungheedae-ro, Seoul 02447, Republic of Korea
2   Lineplant Dental Clinic, 151 Yangji-ro, Gyeyang-gu, Incheon 21016, Republic of Korea
*   Correspondence: swc2007smc@khu.ac.kr

Abstract: Although nickel–titanium (NiTi) rotary files are invaluable tools in dentistry, the relationship between their properties and performance has not been elucidated. Herein, the performance of gold heat-treated (ProTaper Gold and ProfaTaper Gold), controlled memory (CM)-wire (HyFlex CM and V Taper 2H), T-wire (2Shape), and R-phase heat-treated (K3XF) NiTi files was evaluated; the non-heat-treated ProFile was used as the control. The bending, buckling, cyclic fatigue, and torsional resistances of the NiTi files were determined, and their phase transformation behavior was studied through differential scanning calorimetry (DSC). The angle of rotation until fracture (ARF), ultimate torsional strength (UTS), and stiffness were evaluated via torsional resistance testing. One-way analysis of variance (ANOVA) and post hoc analyses were conducted using the Games–Howell test and Tukey's test. ProFile displayed the highest buckling resistance (8 N), CM-wire NiTi files exhibited the lowest bending resistance (0.660–0.758 N cm), and HyFlex CM displayed the highest cyclic fatigue resistance. ProTaper Gold exhibited high UTS and low ARF. K3XF demonstrated high bending resistance and the lowest cyclic fatigue resistance. The CM-wire NiTi files were the most suitable for use in curved canals, while the gold-wire NiTi files were ideal for constricted canals. ProFile was recommended for use in re-treatment cases.

Keywords: bending resistance; buckling resistance; cyclic fatigue; dentistry; differential scanning calorimetry; endodontics; mechanical testing; NiTi file; torsional resistance

1. Introduction

Nickel–titanium (NiTi) rotary files have become essential tools for root canal treatment owing to their higher flexibility and centering and cutting efficiencies than those of stainless-steel hand instruments [1,2]. However, the separation of NiTi files during canal shaping remains a concern for clinicians [3]. To prevent fracture and separation, numerous novel NiTi files have been developed, varying in design, rotation kinematics, and fabrication methods, for which various heat-treatment schemes, surface processing techniques, and electrical discharge machining methods have been applied [4–7].

The mechanical properties of NiTi alloys, and in turn those of NiTi instruments, are closely related to the phase composition of the alloys after heat treatment [8,9]. Depending on the temperature, NiTi alloys can have two different crystalline structures: austenite (high-temperature phase) and martensite (low-temperature phase) [8,10]. The austenite phase is hard and stiff, whereas the martensite phase is ductile and flexible [8,11]. The martensite phase of the NiTi alloy transforms to austenite upon heating [8]. The austenitic phase transformation terminates above a certain temperature, which is known as the austenitic transformation finish temperature (A_f) [8]. Because the A_f of conventional NiTi files is $\leq 22\ ^\circ C$, they are entirely composed of austenite at 22–37 °C. M-wire (Dentsply Tulsa Dental Specialties, Tulsa, OK, USA), a novel NiTi alloy, was developed in 2007 through a specific thermomechanical treatment [5]. At 22 °C, M-wire consists of three phases: deformed and

micro-twinned martensite, R-phase, and austenite. The R-phase is an intermediate phase between austenite and martensite; it has a lower elastic modulus than martensite [8,12]. M-wire exhibits superelasticity and shape memory effects similar to those of conventional NiTi alloys but is more flexible and resistant to cyclic fatigue fracture [8,13,14]. In 2008, R-phase heat treatment was first conducted by SybronEndo (Orange, CA, USA) for the manufacture of Twisted File (SybronEndo). Twisted File was fabricated by twisting R-phase wires instead of grinding them, which led to enhanced flexibility and increased cyclic fatigue resistance in relation to those of a conventional NiTi file (ProFile; Dentsply Maillefer, Ballaigues, Switzerland) [15]. Unlike Twisted File, K3XF (Kerr Dental, Orange, CA, USA) is manufactured via a traditional grinding process, followed by post-machining R-phase heat treatment [10]. K3XF exhibits higher flexibility and resistance to cyclic fatigue than K3 [16], which has an identical design but does not undergo R-phase heat treatment. K3 presents one endothermic peak during austenitic transformation, whereas K3XF displays two peaks and has a higher A_f [17]. According to differential scanning calorimetry (DSC) results, Twisted File and K3XF consist of austenite, martensite, and R-phase at 22 °C [17,18]. R-phase NiTi files display superelasticity and shape memory effects similar to those of M-wire NiTi files [8].

Controlled memory (CM)-wires, introduced in 2010, are thermomechanically treated NiTi wires with a lower nickel content (52 wt.%) than that of conventional NiTi files [19–21]. In contrast to conventional NiTi, M-wire, and R-phase alloys, CM-wires do not display superelasticity. Thus, when an external force bends CM-wire NiTi files, they do not return to their original position when the force is removed [7]. The A_f of CM-wires is 31–55 °C [9,19,22,23]. At room temperature, CM-wires contain a higher martensite content than M-wire or R-phase alloys [15]. NiTi files manufactured using CM-wires outperform conventional, M-wire, and R-phase-wire NiTi files in terms of flexibility and cyclic fatigue resistance at room temperature [9,24–28]. Furthermore, CM-wire NiTi files exhibit higher cyclic fatigue resistance than conventional, C-wire, and T-wire NiTi files at body temperature [28,29]. Although the angle of rotation to fracture (ARF) in torsional fracture resistance tests is higher in CM-wire NiTi files [14,18,25,30], their ultimate torsional strength (UTS) is lower than those of conventional NiTi files [18,25,26,30].

Gold heat-treated files exhibit reduced superelasticity, similar to CM-wire files. Although the manufacturer has not disclosed the exact process of proprietary heat treatment, gold-wire NiTi files appear golden after thermomechanical treatment [7]. According to DSC results, gold-wire NiTi files are mainly composed of martensite and R-phase at room and body temperature [31,32]. The A_f of gold-wire NiTi files is 49–52 °C [31,32]. Additionally, some studies have shown that gold-wire NiTi files exhibit enhanced flexibility and superior cyclic fatigue resistance in relation to conventional files [32,33].

2Shape (Micro-mega, Besançon, France) is a brand that fabricates files through heat treatment using T-wire technology. According to the manufacturer, T-wire heat treatment improves resistance to cyclic fatigue and enhances flexibility [34]. The asymmetrical cross-sectional design of 2Shape files, comprising two main cutting edges and one secondary cutting edge, reduces fracture risk and promotes debris removal [34].

The goal of this study is to determine and compare the bending, buckling, cyclic fatigue, and torsional resistances of six types of heat-treated NiTi files with triangular cross-sectional shapes. ProFile, which is not fabricated via heat treatment, is used as the control. DSC was performed to analyze the phase transformation behavior of the tested NiTi files.

2. Materials and Methods

NiTi files with a tip size of #25 and length of 21 mm were used (Table 1). ProFile, HyFlex CM (Coltene/Whaledent AG, Altstätten, Switzerland), 2Shape, and K3XF have a constant 6% taper, whereas ProTaper Gold (Dentsply Maillefer, Ballaigues, Switzerland), ProfaTaper Gold (Shenzhen Perfect Medical Instruments Co., Ltd., Guangdong, China), and V Taper 2H (SS White Dental, Lakewood, NJ, USA) have variable tapers (Table 1).

Table 1. NiTi files evaluated in this study.

NiTi File	Manufacturer	Tip Size, Taper	Heat Treatment
ProFile	Dentsply Maillefer, Ballaigues, Switzerland	#25, 6%	Conventional wire (no heat treatment)
ProTaper Gold	Dentsply Maillefer, Ballaigues, Switzerland	#25, variable 8% (F2)	Gold-wire
ProfaTaper Gold	Shenzhen Perfect Medical Instruments Co., Ltd., Guangdong, China	#25, variable 8% (T2)	Gold-wire
HyFlex CM	Coltene/Whaledent AG, Altstätten, Switzerland	#25, 6%	CM-wire
V Taper 2H	SS White Dental, Lakewood, NJ, USA	#25, variable 6%	CM-wire
2Shape	Micro-Mega, Besançon, France	#25, 6% (TS2)	T-wire
K3XF	Kerr Dental, Orange, CA, USA	#25, 6%	R-phase

ProFile is a conventional NiTi file [10]. ProTaper Gold and ProfaTaper Gold are manufactured via gold heat treatment [10]. HyFlex CM and V Taper 2H are manufactured using CM-wires [10]. 2Shape is manufactured using T-wire [34], and K3XF is processed by applying the R-phase heat treatment [10].

2.1. Mechanical Tests

Bending, buckling, cyclic fatigue, and torsional fracture resistance tests were performed to assess the mechanical properties of the files. Bending resistance testing was performed in accordance with ISO3630-1:2019 using a universal testing machine (UTM: Universal Mechanics Analyzer, IB Systems, Seoul, Korea) (Figure 1A,B) [35], which consisted of a stainless steel chuck in the upper part and a holding device in the lower part. The UTM included a load cell and a torque sensor for measuring force and torque in real time. The file was gripped at a distance of 3 mm from the tip before being bent horizontally at a point 10 mm away from the grip with a metal arm at a speed of 2 rpm (12 degrees/s). The torque magnitude that induced horizontal bending at 45° was obtained as the bending resistance (N cm) [26].
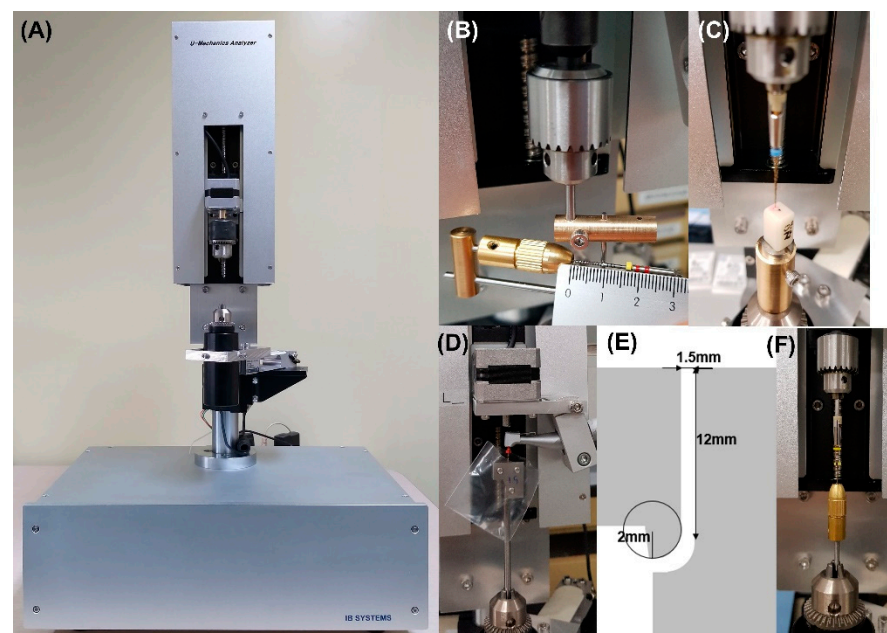
Figure 1. Experimental setup for mechanical testing. (**A**) A universal testing machine (Universal Mechanics Analyzer). Test setup for (**B**) bending, (**C**) buckling, and (**D**) cyclic fatigue resistance tests. (**E**) Schematic of the artificial canal used in the cyclic fatigue resistance test. (**F**) Test setup for the torsional resistance test.

The buckling resistance test was performed using the UTM and a ceramic block (IPS e.max CAD; Ivoclar Vivadent, Schaan, Liechtenstein) bearing small dimples. By holding the handle at the upper part of the UTM, the NiTi file tip was brought into contact with the dimple on the ceramic block (Figure 1C). The file was moved downward at a speed of 1.2 mm/s while maintaining its position in the dimple without slippage. The buckling resistance (N) was determined by measuring the stress at the point where the file handle moved downward by 1 mm [36].

The cyclic fatigue resistance test was conducted by rotating the NiTi file inside an artificial stainless steel curved canal, which was fixed to the lower part of the UTM (Figure 1D). The artificial canal was 17 mm long and had an inner canal diameter of 1.5 mm, a curvature of 45°, and an inner radius of 2 mm (Figure 1E). An endodontic engine (Aseptico, Inc., Woodinville, WA, USA) connected to the upper part of the UTM was used to operate the NiTi file (Figure 1D). Because force sharply decreases immediately upon fracture, a sudden decline in force was regarded as an indication of file fracture. The NiTi files were continuously rotated at 300 rpm, as recommended by the manufacturer. Each NiTi file was rotated until the file broke, and the time to fracture was recorded. The number of cycles to failure (NCF) was calculated by multiplying the time to fracture (minute) by the applied rpm.

The torsional fracture resistance test was performed according to ISO3630-1:2019 [35]. The shaft of the NiTi file was fixed to the upper part of the UTM. The file tip was then tightly clamped into a chuck connected to the lower part of the UTM (Figure 1F). The file was rotated clockwise at 2 rpm (12°/s) until fracture. The rotation angle and torque were automatically recorded using a computer connected to the UTM. The angle of rotation at which the NiTi file fractured was recorded as the ARF (degrees), and the maximum measured torque at the time of fracture was recorded as the UTS (N mm). The torque was plotted against the rotation angle, and the stiffness (N mm/degrees) was calculated from the slope of the linear portion of the graph.

The fractured files were examined through field emission scanning electron microscopy (FE-SEM; JSM-7800F Prime; JEOL Ltd., Akishima, Tokyo, Japan) at various magnifications (×200, ×250, and ×1000) to determine the modes of fracture after the cyclic fatigue and torsional fracture resistance tests.

2.2. Statistical Analysis

The data were normally distributed according to the Shapiro–Wilk test. According to Levene's test, the homogeneity of variances was satisfied for NCF, ARF, and UTS, but not for bending and buckling resistances and stiffness. The bending and buckling resistances as well as the stiffness of the seven types of NiTi files were compared using one-way analysis of variance (ANOVA) and the Games–Howell test. NCF, ARF, and UTS were analyzed using one-way ANOVA and Tukey's post hoc test. Pearson correlation analysis was performed for determining the correlation among the results of the mechanical tests, which included bending and buckling resistances, NCF, ARF, UTS, and stiffness. Statistical analysis was performed using SPSS Statistics version 25 (IBM, Armonk, NY, USA) at a 95% significance level (i.e., $p < 0.05$).

2.3. DSC

DSC was performed on two files per brand using a DSC250 instrument (TA Instruments, New Castle, DE, USA). The analysis involved the following steps: heating from 25 to 90 °C, cooling to −90 °C, and reheating to 90 °C at a rate of 10 °C/min. During the temperature sweep, the heat flow of the file was recorded, and phase transformation temperatures were measured.

3. Results

3.1. Mechanical Tests

K3XF displayed the highest bending resistance (1.5 ± 0.2 N cm), followed by ProFile (1.3 ± 0.2 N cm) and ProTaper Gold (1.3 ± 0.1 N cm), with V Taper 2H exhibiting the lowest value (0.7 ± 0.04 N cm) (Figure 2A, Table 2). ProFile exhibited the highest buckling resistance (8 ± 0.8 N), whereas K3XF (3.7 ± 0.4 N) and V Taper 2H (3.6 ± 0.4 N) (Figure 2B, Table 2) had the lowest. HyFlex CM (784 ± 65) exhibited the highest NCF, followed by ProfaTaper Gold (686 ± 64) and V Taper 2H (602 ± 41) (Figure 2C, Table 2). K3XF exhibited the lowest NCF value (319 ± 33). Moreover, V Taper 2H (745 ± 56 degrees) and ProFile (686 ± 42 degrees) had the highest ARF, whereas ProTaper Gold showed the lowest (396 ± 39 degrees) (Figure 2D, Table 2). ProTaper Gold (15.6 ± 1.3 N mm) possessed the highest UTS, whereas HyFlex CM had the lowest (8.5 ± 0.7 N mm) (Figure 2E, Table 2). Furthermore, K3XF displayed the highest stiffness (0.16 ± 0.02 N mm/degrees), whereas HyFlex CM had the lowest (0.03 ± 0.004 N mm/degrees) (Figure 2F, Table 2). Figure 3 depicts representative curves of torque versus rotation angle plotted using data from the torsional resistance test.
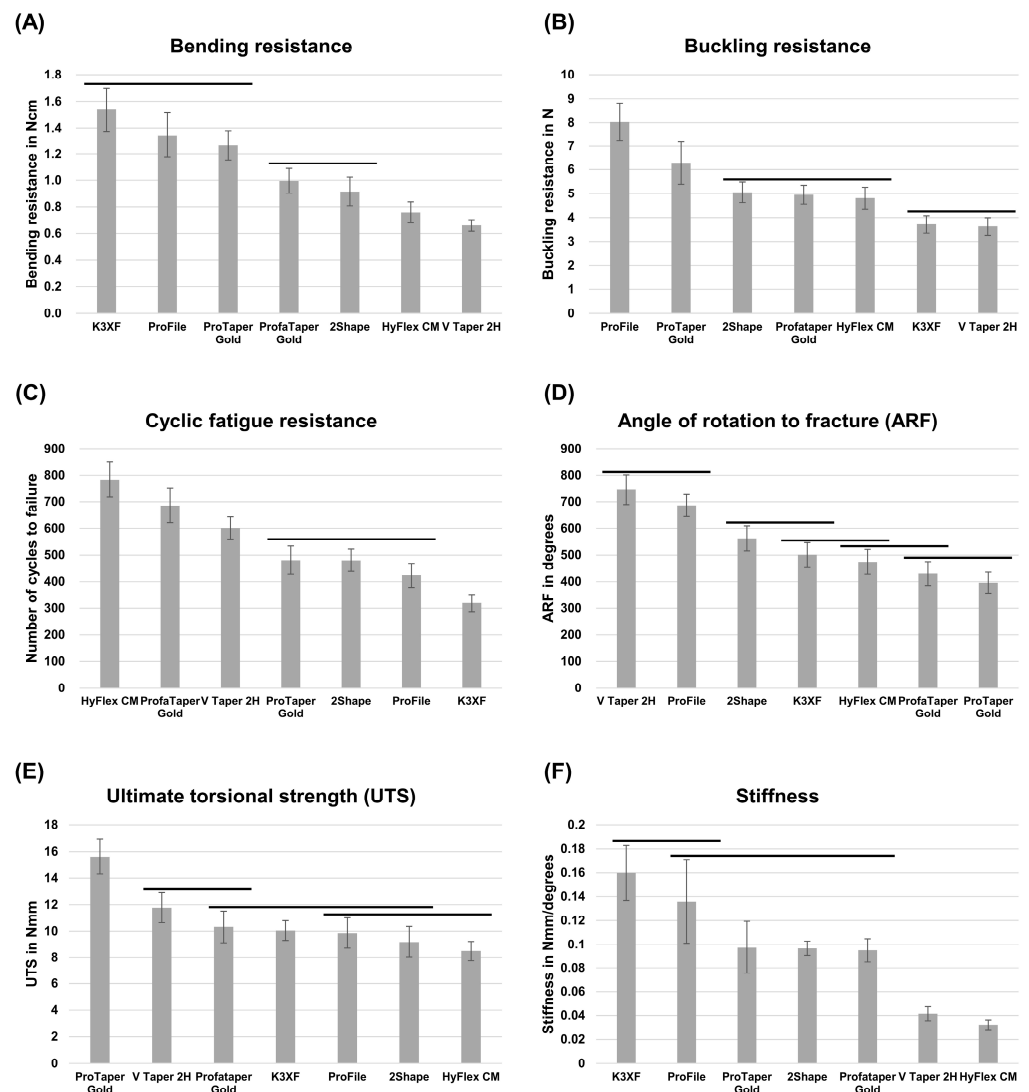

Figure 2. Mechanical test results. (**A**) Bending resistance, (**B**) buckling resistance, (**C**) number of cycles to failure, (**D**) angle of rotation to fracture, (**E**) ultimate torsional strength, and (**F**) stiffness. Groups under the same name bar have no significant difference.

**Table 2.** Mechanical test results. Mean ± standard deviation.

	ProFile	ProTaper Gold	ProfaTaper Gold	HyFlex CM	2Shape	V Taper 2H	K3XF
Bending resistance (N cm)	1.3 ± 0.2 [d]	1.3 ± 0.1 [d]	1 ± 0.1 [c]	0.8 ± 0.1 [b]	0.9 ± 0.1 [c]	0.7 ± 0.04 [a]	1.5 ± 0.2 [d]
Buckling resistance (N)	8 ± 0.8 [d]	6.3 ± 0.9 [c]	5 ± 0.4 [b]	4.8 ± 0.5 [b]	5.1 ± 0.4 [b]	3.6 ± 0.4 [a]	3.7 ± 0.4 [a]
Number of cycles to failure	424 ± 45 [b]	480 ± 53 [b]	686 ± 64 [d]	784 ± 65 [e]	480 ± 42 [b]	602 ± 41 [c]	319 ± 33 [a]
Angle of rotation to fracture (degrees)	686 ± 42 [e]	396 ± 39 [a]	430 ± 45 [a, b]	474 ± 47 [b, c]	562 ± 47 [d]	745 ± 56 [e]	501 ± 45 [c,d]
Ultimate torsional strength (N mm)	9.9 ± 1.1 [a, b]	15.6 ± 1.3 [d]	10.3 ± 1.2 [b, c]	8.5 ± 0.7 [a]	9.2 ± 1.2 [a, b]	11.8 ± 1.1 [c]	10.1 ± 0.7 [b]
Stiffness (N mm/degrees)	0.14 ± 0.03 [c,d]	0.1 ± 0.02 [c]	0.1 ± 0.01 [c]	0.03 ± 0.004 [a]	0.1 ± 0.006 [c]	0.04 ± 0.006 [b]	0.16 ± 0.02 [d]

Different superscript letters in the same row indicate a statistically significant difference ($p < 0.05$).
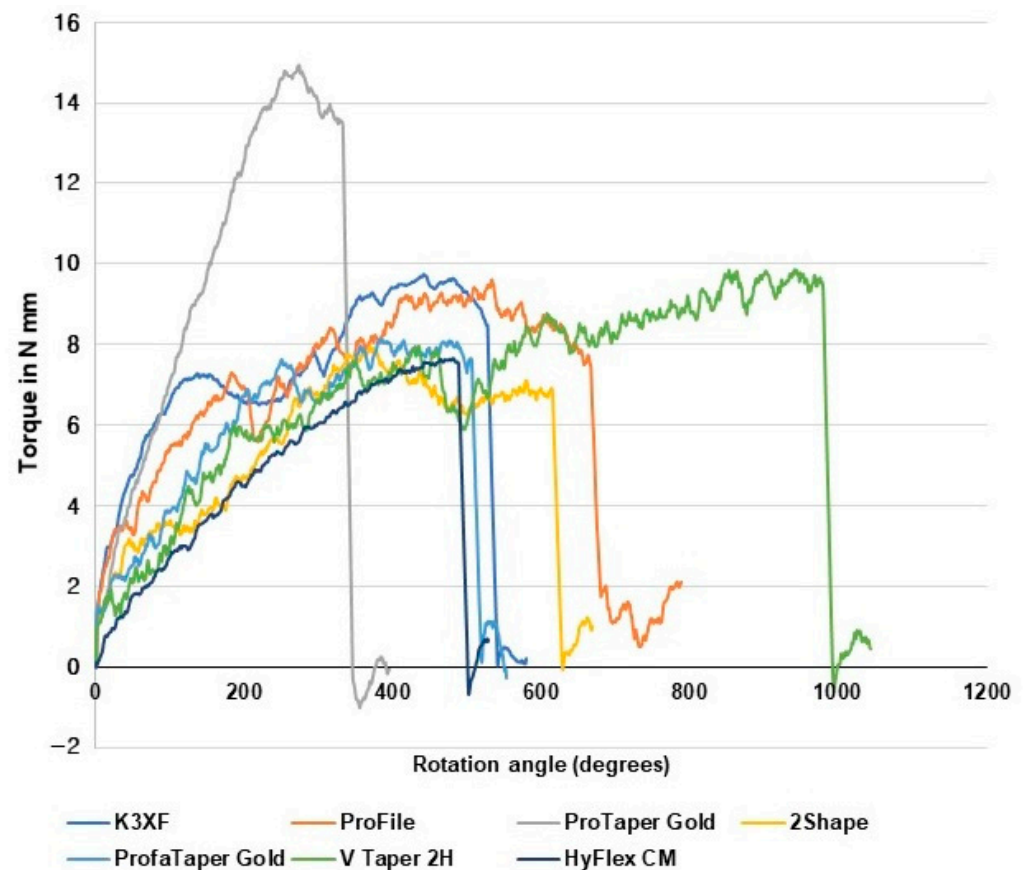
Figure 3. Torque vs. rotational angle plots showing the point of torsional fracture for each NiTi file. The slope of the initial linear portion of the graph was obtained as the stiffness.

The fractured surfaces of the files reveal microcracks in the peripheral region and multiple striations near the microcracks as a result of cyclic fatigue resistance testing (Figure 4). The magnified images of the cross-sections show mixed zones comprising fatigue striations and dimple clusters (Figure 4(A2–G2)). The lateral surfaces of the fractured NiTi files display brittle fractures with cracks (Figure 4). Plastic deformation patterns, such as flute unwinding, were not visible in the fractured files.
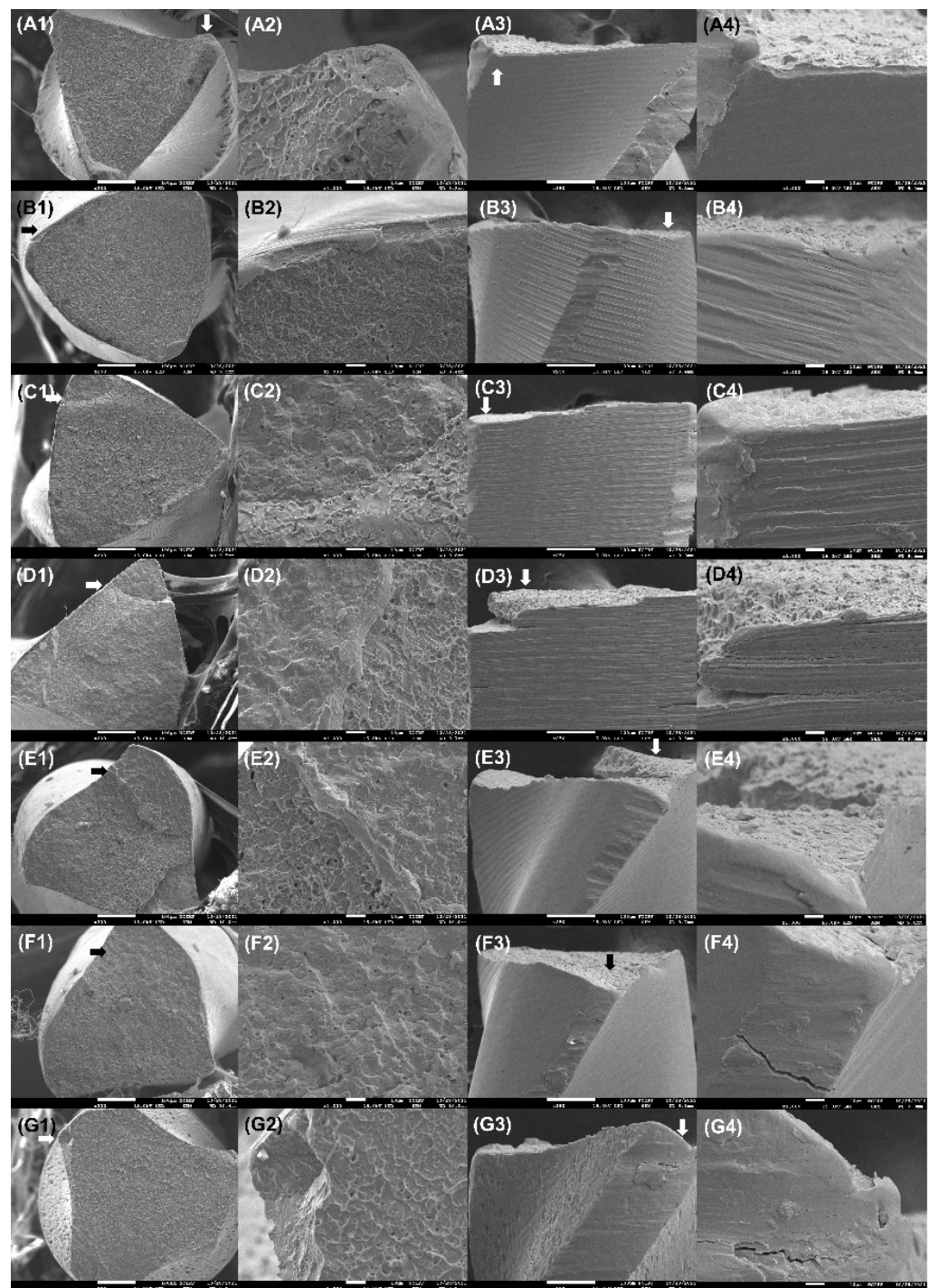
Figure 4. SEM images after cyclic fatigue resistance testing of (**A**) ProFile, (**B**) ProTaper Gold, (**C**) ProfaTaper Gold, (**D**) HyFlex CM, (**E**) V Taper 2H, (**F**) 2Shape, and (**G**) K3XF. (**A1**–**G1**) Fractured surfaces (×200); (**A2**–**G2**) magnified (×1000) images of the fractured surfaces at the arrow regions in (**A1**–**G1**), showing fatigue striations; (**A3**–**G3**) lateral surfaces (×250); (**A4**–**G4**) magnified (×1000) views of fractured surfaces at the arrow regions in (**A3**–**G3**), showing cracks.

The fractured surfaces after the torsional resistance tests exhibit multiple circular abrasion marks at the center of the cross-section (Figure 5(A2–G2). The lateral surfaces of the fractured NiTi files display ductile fractures with plastic deformation (Figure 5).
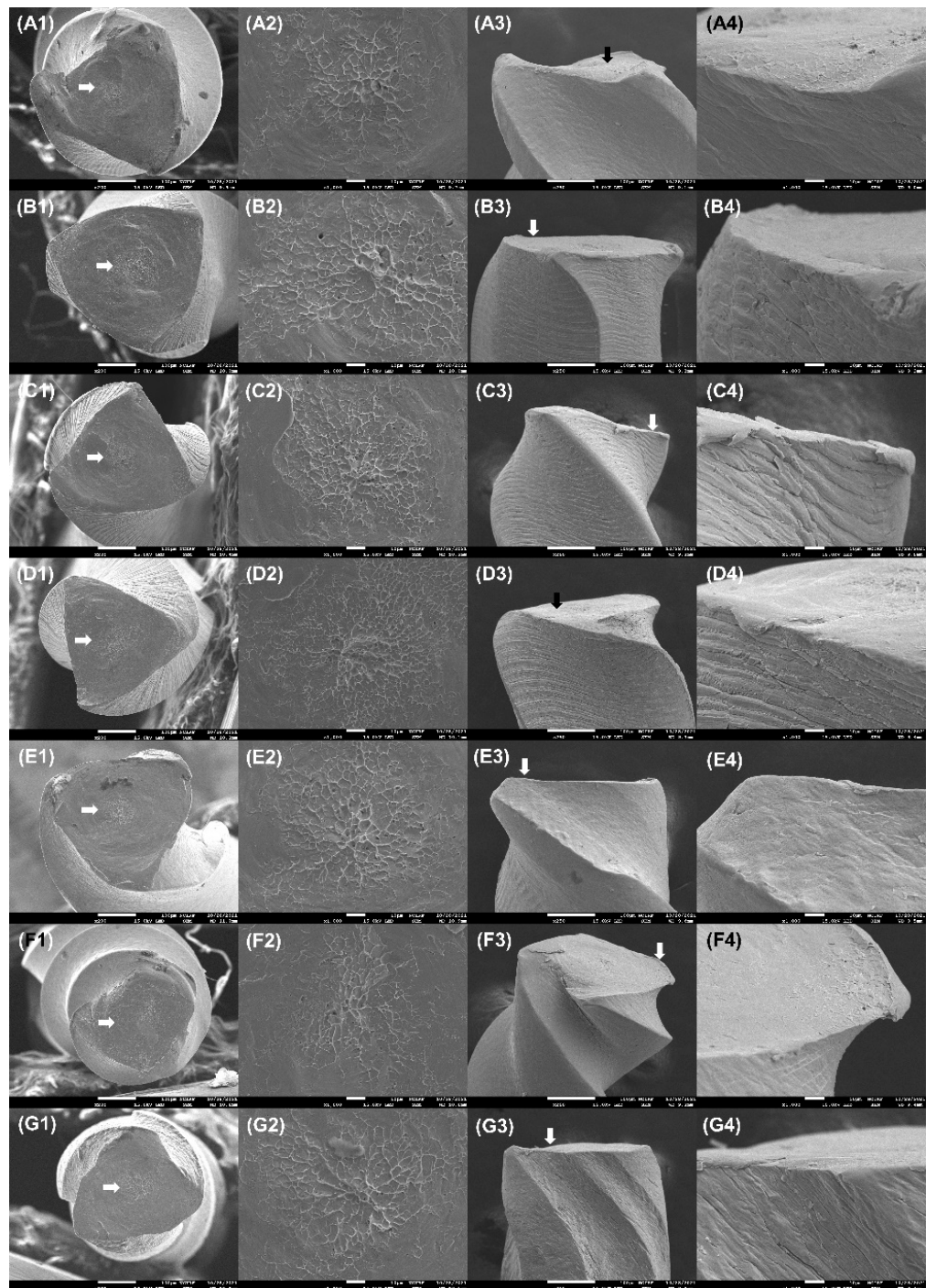
Figure 5. SEM images after the torsional resistance test of (**A**) ProFile, (**B**) ProTaper Gold, (**C**) ProfaTaper Gold, (**D**) HyFlex CM, (**E**) V Taper 2H, (**F**) 2Shape, and (**G**) K3XF. (**A1–G1**) Fractured surfaces (×200); (**A2–G2**) magnified (×1000) view of fractured surfaces at the arrow region in (**A1–G1**), showing circular abrasion marks; (**A3–G3**) lateral surfaces (×250), showing plastic deformation; (**A4–G4**) magnified (×1000) view of fractured surfaces at the arrow regions in (**A3–G3**), indicating the absence of cracks.

3.2. Pearson Correlation Analysis

The bending and buckling resistances displayed a moderately positive correlation ($p < 0.05$, Pearson's r = 0.353). The bending resistance and NCF displayed a strong negative correlation ($p < 0.001$, Pearson's r = −0.72). The bending resistance and stiffness displayed a

strong positive correlation ($p < 0.001$, Pearson's r = 0.829). The stiffness and NCF displayed a strong negative correlation ($p < 0.001$, Pearson's r = −0.772).

3.3. DSC

The DSC profiles of ProFile and 2Shape show single endothermic and exothermic peaks below 22 °C (Figure 6A,F). The DSC curves of ProTaper Gold contain single endothermic and exothermic peaks (Figure 6B), while those of ProfaTaper Gold contain two endothermic peaks and a single exothermic peak above 22 °C (Figure 6C). HyFlex CM and V Taper 2H display a single endothermic and two exothermic peaks (Figure 6D,E). The first exothermic peak in the curve corresponds to the austenite to R-phase transformation, which occurs above 22 °C. The starting temperatures of the martensite to austenitic transformation—which was represented by the endothermic curves—of HyFlex CM and V Taper 2H were above 22 °C (Figure 6D,E). The DSC curves of K3XF present two consecutive endothermic peaks below 22 °C (Figure 6G): the first represents the initial transformation from martensite to the R-phase, and the second indicates the transformation from the R-phase to austenite. The exothermic curve of K3XF presents a single peak below 22 °C (Figure 6G). Table 3 lists the phase transformation temperatures and associated enthalpy changes.
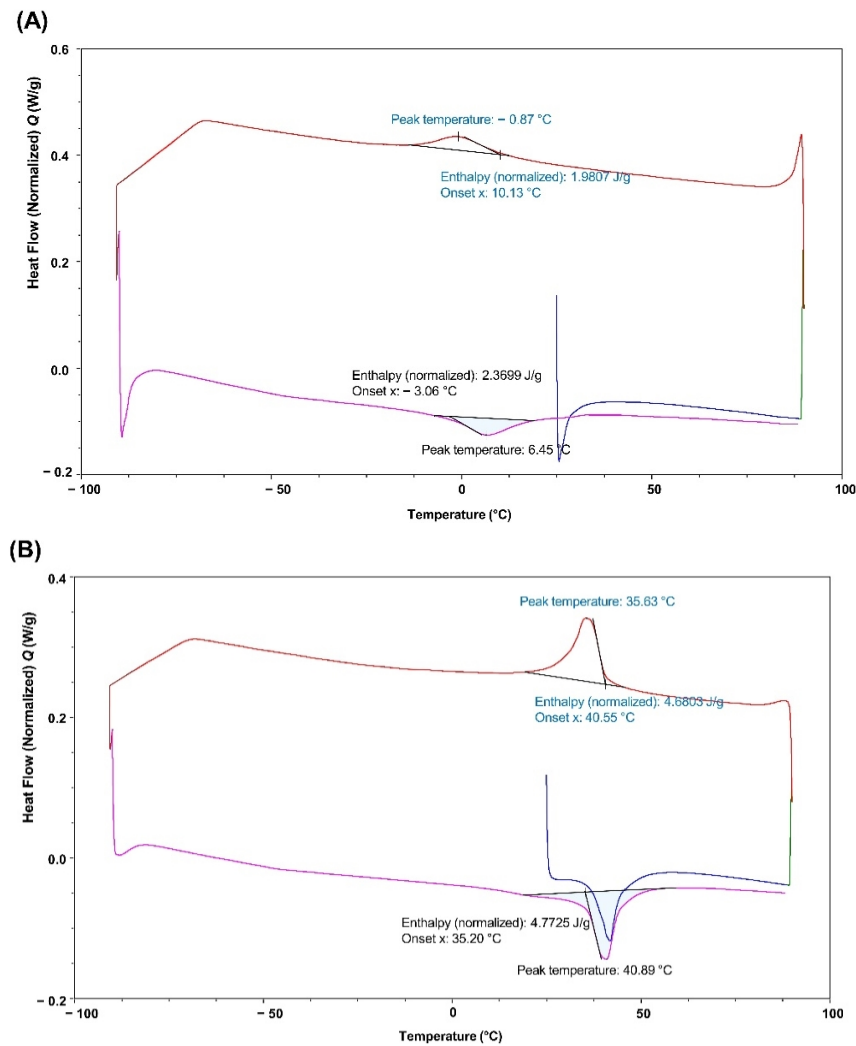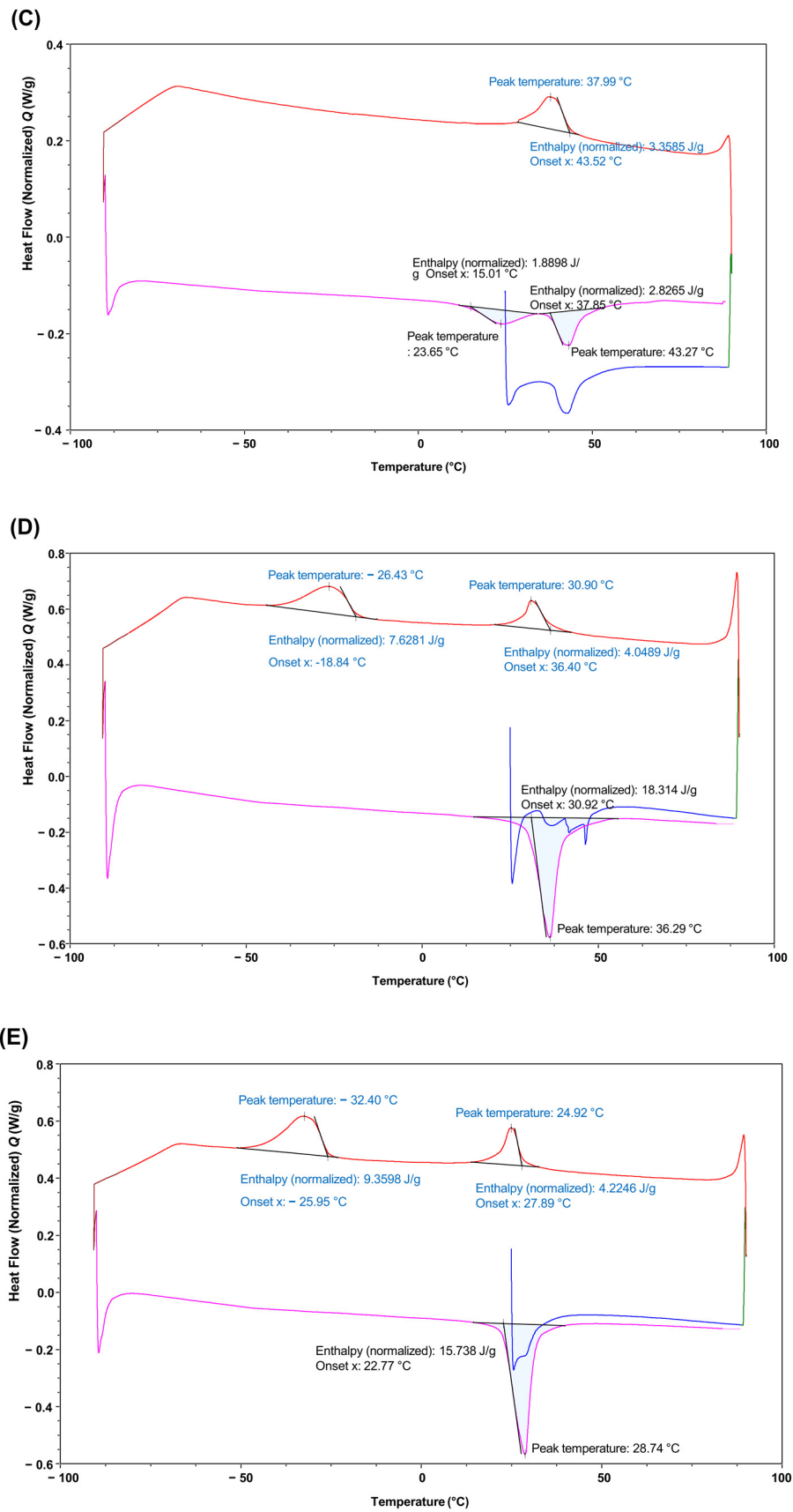
Figure 6. *Cont.*

(C)

(D)

(E)

Figure 6. *Cont.*

(F)

(G)
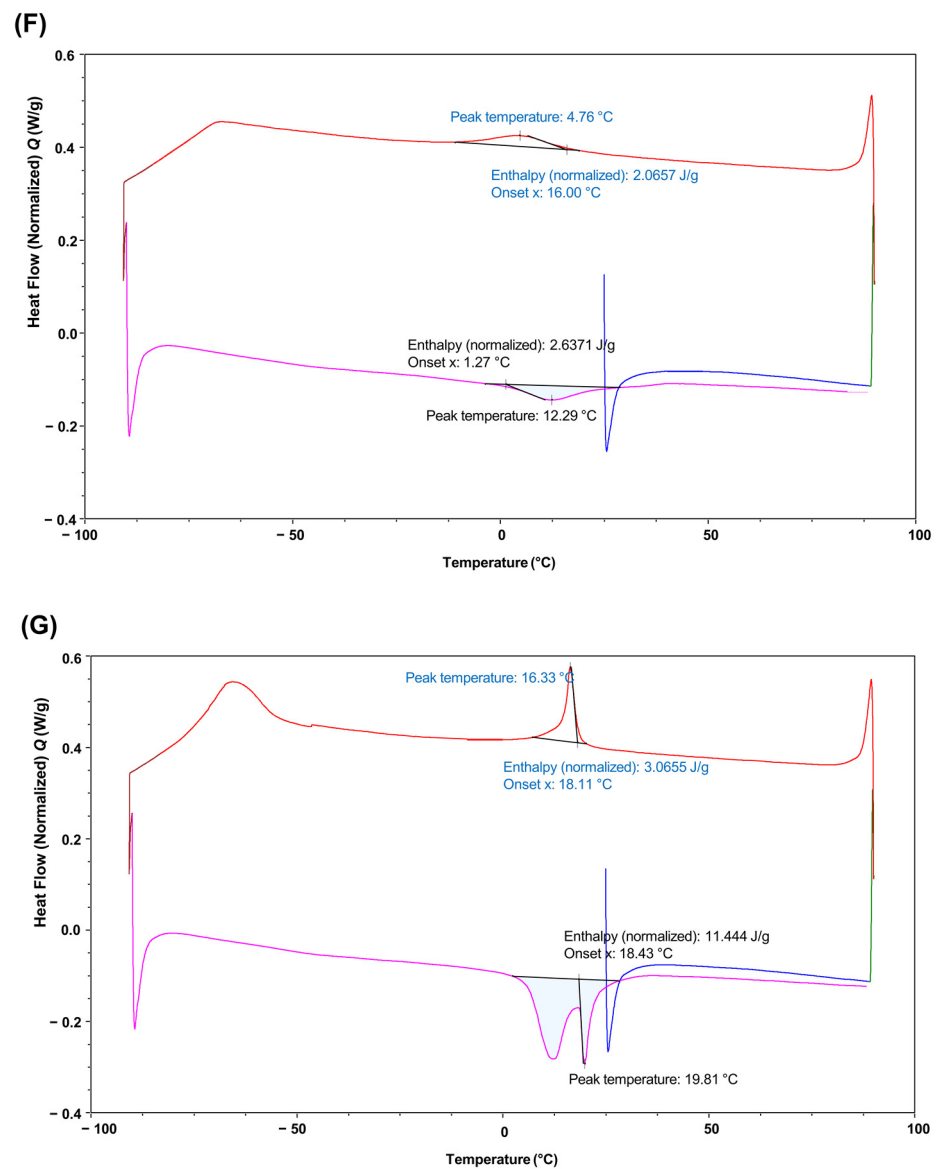
Figure 6. DSC curves of (**A**) ProFile, (**B**) ProTaper Gold, (**C**) ProfaTaper Gold, (**D**) HyFlex CM, (**E**) V Taper 2H, (**F**) 2Shape, and (**G**) K3XF. The upper and lower curves represent the cooling and heating curves, respectively.

Table 3. Phase transformation temperatures and associated enthalpy changes derived from the DSC curves.

	Heating (Endothermic) Curve					
	R_s (°C)	R_f (°C)	ΔH (J/g)	A_s (°C)	A_f (°C)	ΔH (J/g)
ProFile				−3.06	19.27	2.37
ProTaper Gold				35.20	47.92	4.77
ProfaTaper Gold	15.01	36.46	1.89	37.85	56.25	2.83
HyFlex CM				30.92	58.33	18.31
V Taper 2H				22.77	41.67	15.74
2Shape				1.27	29.69	2.64
K3XF	2.08	18.43		18.43	30.21	11.44 *

Table 3. *Cont.*

	Cooling (Exothermic) Curve					
	R_s (°C)	R_f (°C)	ΔH (J/g)	M_s (°C)	M_f (°C)	ΔH (J/g)
ProFile				10.13	−13.54	1.98
ProTaper Gold				40.55	19.79	4.68
ProfaTaper Gold				43.52	29.17	3.36
HyFlex CM	36.40	21.35	4.05	−18.84	−46.35	7.63
V Taper 2H	27.89	14.58	4.22	−25.95	−53.44	9.36
2Shape				16.00	−11.46	2.07
K3XF				18.11	6.77	3.07

R_s and R_f are the start and finish temperatures, respectively, of the R-phase transformation. A_s and A_f are the start and finish temperatures, respectively, of the austenitic transformation. M_s and M_f are the start and finish temperatures, respectively, of the martensitic transformation. * represents the total energy of the martensite to R-phase and R-phase to austenitic transformations.

4. Discussion

The mechanical properties of the NiTi files were assessed using four tests. The bending resistance test evaluated the flexibility of the NiTi file, with lower bending resistance indicating superior flexibility. The CM-wire NiTi files, HyFlex CM and V Taper 2H, demonstrated superior flexibility, which is consistent with previous research findings [9,19,26]. Among the tested NiTi files, the CM-wire NiTi files exhibited no superelasticity, while the gold-wire NiTi files exhibited lower superelasticity. After bending the CM-wire NiTi files to 45°, the residual angle was nearly 45° even after the external force was removed. By contrast, the gold-wire NiTi files displayed spring-back behavior after the removal of the bending force. In addition, the larger cross-sectional area of ProTaper Gold and ProfaTaper Gold contributed to their higher bending resistances than those of HyFlex CM and V Taper 2H.

The buckling resistance of a file is its capacity to resist sideways deflection when the compressive load exceeds the resistance of the file [37]. However, there is no standard for testing the buckling resistance in NiTi files. Lopes et al. [37] measured buckling resistance as the force generated by a 1 mm lateral elastic displacement. In our study, we measured buckling resistance as the force generated by a 1 mm vertical (downward) displacement, because the lateral displacement could not be measured. Herein, ProFile exhibited the highest buckling resistance. The DSC results showed that ProFile is composed of austenite at 22 °C (Figure 6A), which explains its buckling behavior because the stiffness and hardness of austenite are higher than those of martensite [10,11]; therefore, an austenite-rich NiTi file more effectively resists sideways deflection by a compressive load. Buckling resistance can be used to assess the penetrating ability of NiTi files. The orifice of the root canal is often narrow and calcified, and any instrument used must be capable of penetrating it [38]. Furthermore, during re-treatment, gutta-percha and root canal sealers should be removed. NiTi files with a high buckling resistance are suitable for penetrating any previous root canal filling materials that may be present. ProFile comprises three radial lands and U-shaped flutes, whereas the cross-sectional shape of ProTaper Gold is convex and triangular without radial lands (Figure 4A,B). Thus, the ProFile shape facilitates more efficient removal of old filling materials and debris toward the orifice of the root canal.

According to the results of the Pearson correlation analysis, the bending and buckling resistances were moderately positively correlated. HyFlex CM and V Taper 2H exhibited low bending and buckling resistances (Figure 2A,B). Therefore, these flexible NiTi files are ideal for operating on curved root canals [39,40]. Meanwhile, HyFlex CM had the lowest UTS among the tested NiTi files, and the stiffness of V Taper 2H and HyFlex CM was lower than that of other NiTi files because of their high martensite content. Therefore, extreme caution should be taken when using these files to shape a narrow, calcified canal.

K3XF exhibited the highest bending resistance, but its buckling resistance was low (Figure 2A,B). K3XF has a larger number of threads and a constant 6% taper. The volume of the K3XF file in the 3 mm tip is lower than those of ProTaper Gold and ProfaTaper Gold. The small volume of K3XF possibly resulted in its lower buckling resistance.

NiTi file fracture occurs because of cyclic and torsional fatigue. Cyclic fatigue fractures result from the repetitive compressive and tensile stresses that occur when the NiTi file is rotated inside a curved canal [41]. Torsional fractures occur when the file tip is locked in a canal while the shaft continues to rotate [41]. Cyclic fatigue resistance is related to the flexibility of the NiTi file [18]. According to the results of the Pearson correlation analysis, the bending resistance and NCF had a strong negative correlation, indicating that the more flexible the NiTi file, the more resistant it was to cyclic fatigue fracture. HyFlex CM had the highest NCF, followed by ProfaTaper Gold and V Taper 2H (Figure 2C), which is consistent with previous research findings that martensitic NiTi files, such as CM-wire NiTi files, exhibit superior cyclic fatigue resistance [24–29]. In this study, K3XF exhibited the lowest NCF, even lower than that of ProFile, the non-heat-treated NiTi file (Figure 2C). K3XF was mostly in its austenite phase during the cyclic fatigue resistance test, which was performed at 22 °C (Figure 6G). The cross-sectional area of K3XF was larger than that of ProFile (Figure 4A,G), which contributed to its lower cyclic fatigue resistance. A previous study using NiTi files with 4% taper and #25 tip size reported that the cyclic fatigue resistance of K3XF is comparable to that of ProFile and lower than that of HyFlex CM at 22 °C and 37 °C, respectively [42]. The disparity between the results of the previous study and our study was caused by the different sizes of the tested NiTi files.

Torsional fracture resistance is defined by both the ARF and UTS of a material. V Taper 2H had the largest ARF (Figure 2D) despite having the lowest bending and buckling resistances (Figure 2A,B). According to its torque versus rotation angle plot, V Taper 2H underwent significant plastic deformation after elastic deformation (Figure 3). Overall, V Taper 2H was the least resistant to lateral and vertical compressive loads, but more resistant to continuous rotation stresses. Furthermore, V Taper 2H had the second highest UTS, while HyFlex CM, another brand of the CM-wire NiTi file, had the lowest. The superior torsional resistance of the V Taper 2H file is presumably due to design features such as a larger number of threads and a modified triangular cross-section [43]. ProFile displayed the second largest ARF after V Taper 2H, with the values differing to a small degree (Figure 2D). The small cross-sectional area resulting from the U-shaped flute is considered to contribute to the larger ARF of ProFile than that of most other NiTi files.

ProTaper Gold exhibited the highest UTS and lowest ARF values (Figure 2D,E). The larger the ARF of a NiTi file, the greater its elastic and plastic deformation before separation [44]. The UTS and ARF are possibly affected by the core mass of NiTi files. ProTaper Gold presents an 8% taper at the 3 mm tip region and has a convex triangular cross-section, granting it more metal mass in the 3–4 mm tip region than any other NiTi file tested in this study. This finding is in agreement with the previously reported results, which confirmed that a larger cross-sectional area contributes to a higher bending resistance and UTS [26,45,46]. NiTi files with low ARF values, such as ProTaper Gold and ProfaTaper Gold, may not provide sufficient warning signs, such as permanent deformation, before fracture [44]. Based on these results, ProTaper Gold is recommended for use in calcified and/or straight canals. It is suggested to discard the ProTaper Gold file after use for a severely calcified root canal rather than reuse it in the remaining root canal of a tooth.

The bending and buckling resistances of ProfaTaper Gold were lower than those of ProTaper Gold (Figure 2A,B). ProfaTaper Gold exhibited higher cyclic fatigue resistance than ProTaper Gold, as represented by the NCF value (Figure 2C). The ARFs of ProfaTaper Gold and ProTaper Gold were not significantly different (Figure 2D), but ProfaTaper Gold exhibited a lower UTS than ProTaper Gold (Figure 2E). Although ProfaTaper Gold is a counterfeit version of ProTaper Gold, the cross-sectional shapes of the two files differ. ProTaper Gold has a more convex cross-section with a larger cross-sectional area than ProfaTaper Gold (Figures 4B1,C1 and 5B1,C1), which contribute to its higher bending

and buckling resistances, higher UTS, and lower cyclic fatigue resistance. Additionally, according to the heating curve in the DSC profiles of ProfaTaper Gold (Figure 6C), a mixture of austenite, martensite, and R-phase exists at 22 °C. Because the elastic modulus of the R-phase is lower than those of austenite and martensite [47], NiTi files comprising the R-phase are more flexible and less resistant to bending and buckling.

The stiffness values of V Taper 2H and HyFlex CM were the lowest, differing only marginally (Figure 2F). A low stiffness indicates lower resistance to continuous clockwise rotation. Stiffness was found to be positively correlated with the bending resistance ($p < 0.001$, Pearson's r = 0.829), which is a measure of the resistance to bending in the direction perpendicular to the long axis of the NiTi file. V Taper 2H and HyFlex CM underwent a two-phase transformation during cooling, as indicated by their DSC curves (Figure 6D,E). The CM-wire NiTi files, V Taper 2H and HyFlex CM, presented low stiffness and high flexibility at 22 °C owing to their martensite and R-phase composition.

At 22 °C, 2Shape was primarily composed of austenite. In this study, the flexibility of 2Shape was found to be higher than that of ProFile and lower than that of the CM-wire NiTi files. The NCF of 2Shape was comparable to that of ProFile and lower than those of CM-wire NiTi files, which is consistent with the results of a previous study [28]. The flexibility and cyclic fatigue resistance were mostly affected by heat treatment applied during manufacturing. The ARF of 2Shape was lower than those of ProFile and V Taper 2H. As a superelastic NiTi file, 2Shape exhibited lower ductility than V Taper 2H. By contrast, the ARF of 2Shape was larger than those of HyFlex CM, ProfaTaper Gold, and ProTaper Gold. The ARF of 2Shape is considered to be larger due to its small cross-sectional area, which results from its asymmetrical modified triangular shape. By contrast, the small cross-sectional area contributed to the lower UTS of 2Shape. Hence, it is recommended to use 2Shape in straight or slightly curved root canals.

The mechanical tests in this study were conducted at 22 °C. In the heating curves of the DSC profiles, the peak temperatures attributed to the austenitic transformations of ProTaper Gold, ProfaTaper Gold, HyFlex CM, and V Taper 2H were 40.89, 43.27, 36.29, and 28.74 °C, respectively (Figure 6B,C,D,E, respectively). Evidently, the phase composition of these NiTi files varies with increasing environmental temperature from 22 to 37 °C. Previous studies have reported that cyclic fatigue resistance decreases at elevated testing temperatures [12,31,42]. Therefore, further studies on the bending, buckling, cyclic fatigue, and torsional resistances of NiTi files at body temperature are needed.

One of the limitations of our study is that the phase transitions of NiTi files were not studied in real time through in situ crystallography based on X-ray diffraction. Instead, we performed DSC, which provides limited information, to elucidate the possible metallurgical features of the samples. The DSC results combined with the data from the literature were sufficient to verify our main findings and hypotheses. Another drawback is that this study establishes weak correlations between the tested mechanical properties, which makes it difficult to draw decisive conclusions about possible clinical implications.

2Shape was operated utilizing two file systems: TS1 (#25/04) followed by TS2 (#25/06), up to the working length. ProFile, HyFlex CM, and K3XF were intended for use with a crown-down technique. ProTaper Gold and ProfaTaper Gold instructions mandated the sequential use of four to five files along the working length. V Taper 2H instructions stated that it should be used in conjunction with a glide path-preparing file, followed by #20/04 and #25/06 for the working length. The amount of dentin removed during canal shaping varies depending on the NiTi file brand, as does the amount of stress generated by the NiTi files. The cutting, centering, and debris removal efficiencies of each file during canal shaping should be investigated further.

Interaction between a titanium implant and metal prosthesis may induce galvanic corrosion, ion release, and peri-implantitis [48]. Nickel release from orthodontic brackets has been widely reported, which is an issue that requires attention due to the possibility of allergic reactions in patients [49]. Therefore, the mechanisms underlying ion release from NiTi files manufactured through different heat treatments must be investigated.

This study revealed that CM-wire NiTi files have superior flexibility and exhibit high cyclic fatigue resistance. Although the cross-sectional shapes of all tested files are triangular or the files have modified triangular cross-sections, their mechanical properties vary depending on the heat treatment type. More research, however, is required to further our understanding of the differences in the characteristics of CM-wire, gold-wire, T-wire, and R-phase wire.

5. Conclusions

This study showed that CM-wire NiTi files outperformed the other tested files in curved canals because of their superior flexibility and high cyclic fatigue resistance. Gold-wire NiTi files are best suited for use in constricted canals as they exhibited the highest UTS. ProFile is recommended for use in re-treatment cases as it exhibited high buckling and bending resistances. 2Shape, a T-wire NiTi file, is recommended for use in slightly curved canals. K3XF is better suited for use in straight rather than curved root canals.

Author Contributions: Conceptualization, T.-H.K. and S.W.C.; methodology, S.O. and T.-H.K.; software, S.O.; validation, T.-H.K. and S.W.C.; formal analysis, S.O. and T.-H.K.; investigation, S.O. and T.-H.K.; resources, S.W.C.; data curation, S.O. and T.-H.K.; writing—original draft preparation, S.O. and T.-H.K.; writing—review and editing, S.W.C.; supervision, S.W.C.; project administration, S.O. and T.-H.K.; funding acquisition, S.O. and T.-H.K. contributed equally to this work. All authors have read and agreed to the published version of the manuscript.

Institutional Review Board Statement: Not applicable.

Informed Consent Statement: Not applicable.

Data Availability Statement: The data presented in this study are available upon request from the corresponding author.

Conflicts of Interest: The authors declare no conflict of interest.

References

1. Celik, D.; Taşdemir, T.; Er, K. Comparative study of 6 rotary nickel-titanium systems and hand instrumentation for root canal preparation in severely curved root canals of extracted teeth. *J. Endod.* **2013**, *39*, 278–282. [CrossRef]
2. Cheung, G.S.; Liu, C.S. A retrospective study of endodontic treatment outcome between nickel-titanium rotary and stainless steel hand filing techniques. *J. Endod.* **2009**, *35*, 938–943. [CrossRef] [PubMed]
3. Wu, J.; Lei, G.; Yan, M.; Yu, Y.; Yu, J.; Zhang, G. Instrument separation analysis of multi-used ProTaper Universal rotary system during root canal therapy. *J. Endod.* **2011**, *37*, 758–763. [CrossRef]
4. Caballero-Flores, H.; Nabeshima, C.K.; Binotto, E.; Machado, M.E.L. Fracture incidence of instruments from a single-file reciprocating system by students in an endodontic graduate programme: A cross-sectional retrospective study. *Int. Endod. J.* **2019**, *52*, 13–18. [CrossRef] [PubMed]
5. Gambarini, G.; Grande, N.M.; Plotino, G.; Somma, F.; Garala, M.; De Luca, M.; Testarelli, L. Fatigue resistance of engine-driven rotary nickel-titanium instruments produced by new manufacturing methods. *J. Endod.* **2008**, *34*, 1003–1005. [CrossRef] [PubMed]
6. Keskin, N.B.; Inan, U. Cyclic fatigue resistance of rotary NiTi instruments produced with four different manufacturing methods. *Microsc. Res. Tech.* **2019**, *82*, 1642–1648. [CrossRef]
7. Tabassum, S.; Zafar, K.; Umer, F. Nickel-Titanium rotary file systems: What's new? *Eur. Endod. J.* **2019**, *4*, 111–117. [CrossRef]
8. Shen, Y.; Zhou, H.M.; Zheng, Y.F.; Peng, B.; Haapasalo, M. Current challenges and concepts of the thermomechanical treatment of nickel-titanium instruments. *J. Endod.* **2013**, *39*, 163–172. [CrossRef] [PubMed]
9. Braga, L.C.; Silva, A.C.F.; Buono, V.T.; de Azevedo Bahia, M.G. Impact of heat treatments on the fatigue resistance of different rotary nickel-titanium instruments. *J. Endod.* **2014**, *40*, 1494–1497. [CrossRef]
10. Zupanc, J.; Vahdat-Pajouh, N.; Schäfer, E. New thermomechanically treated NiTi alloys—A review. *Int. Endod. J.* **2018**, *51*, 1088–1103. [CrossRef] [PubMed]
11. Thompson, S.A. An overview of nickel-titanium alloys used in dentistry. *Int. Endod. J.* **2000**, *33*, 297–310. [CrossRef]
12. de Vasconcelos, R.A.; Murphy, S.; Carvalho, C.A.; Govindjee, R.G.; Govindjee, S.; Peters, O.A. Evidence for reduced fatigue resistance of contemporary rotary instruments exposed to body temperature. *J. Endod.* **2016**, *42*, 782–787. [CrossRef] [PubMed]

13. Pereira, E.S.; Gomes, R.O.; Leroy, A.M.; Singh, R.; Peters, O.A.; Bahia, M.G.; Buono, V.T. Mechanical behavior of M-Wire and conventional NiTi wire used to manufacture rotary endodontic instruments. *Dent. Mater.* **2013**, *29*, e318–e324. [CrossRef] [PubMed]

14. Goo, H.J.; Kwak, S.W.; Ha, J.H.; Pedullà, E.; Kim, H.C. Mechanical properties of various heat-treated nickel-titanium rotary instruments. *J. Endod.* **2017**, *43*, 1872–1877. [CrossRef] [PubMed]

15. Bouska, J.; Justman, B.; Williamson, A.; DeLong, C.; Qian, F. Resistance to cyclic fatigue failure of a new endodontic rotary file. *J. Endod.* **2012**, *38*, 667–669. [CrossRef] [PubMed]

16. Gambarini, G.; Plotino, G.; Grande, N.M.; Al-Sudani, D.; De Luca, M.; Testarelli, L. Mechanical properties of nickel-titanium rotary instruments produced with a new manufacturing technique. *Int. Endod. J.* **2011**, *44*, 337–341. [CrossRef] [PubMed]

17. Shen, Y.; Zhou, H.M.; Wang, Z.; Campbell, L.; Zheng, Y.F.; Haapasalo, M. Phase transformation behavior and mechanical properties of thermomechanically treated K3XF nickel-titanium instruments. *J. Endod.* **2013**, *39*, 919–923. [CrossRef]

18. Shim, K.S.; Oh, S.; Kum, K.; Kim, Y.C.; Jee, K.K.; Chang, S.W. Mechanical and metallurgical properties of variou nickel-titanium rotary instruments. *Biomed. Res. Int.* **2017**, *2017*, 4528601. [CrossRef] [PubMed]

19. Zhou, H.M.; Shen, Y.; Zheng, W.; Li, L.; Zheng, Y.F.; Haapasalo, M. Mechanical properties of controlled memory and superelastic nickel-titanium wires used in the manufacture of rotary endodontic instruments. *J. Endod.* **2012**, *38*, 1535–1540. [CrossRef]

20. Testarelli, L.; Plotino, G.; Al-Sudani, D.; Vincenzi, V.; Giansiracusa, A.; Grande, N.M.; Gambarini, G. Bending properties of a new nickel-titanium alloy with a lower percent by weight of nickel. *J. Endod.* **2011**, *37*, 1293–1295. [CrossRef]

21. Zinelis, S.; Eliades, T.; Eliades, G. A metallurgical characterization of ten endodontic Ni-Ti instruments: Assessing the clinical relevance of shape memory and superelastic properties of Ni-Ti endodontic instruments. *Int. Endod. J.* **2010**, *43*, 125–134. [CrossRef]

22. Shen, Y.; Zhou, H.M.; Zheng, Y.F.; Campbell, L.; Peng, B.; Haapasalo, M. Metallurgical characterization of controlled memory wire nickel-titanium rotary instruments. *J. Endod.* **2011**, *37*, 1566–1571. [CrossRef]

23. Chang, S.W.; Shim, K.S.; Kim, Y.C.; Jee, K.K.; Zhu, Q.; Perinpanayagam, H.; Kum, K.Y. Cyclic fatigue resistance, torsional resistance, and metallurgical characteristics of V taper 2 and V taper 2H rotary NiTi files. *Scanning* **2016**, *38*, 564–570. [CrossRef] [PubMed]

24. Shen, Y.; Qian, W.; Abtin, H.; Gao, Y.; Haapasalo, M. Fatigue testing of controlled memory wire nickel-titanium rotary instruments. *J. Endod.* **2011**, *37*, 997–1001. [CrossRef] [PubMed]

25. Pereira, É.S.; Viana, A.C.; Buono, V.T.; Peters, O.A.; Bahia, M.G. Behavior of nickel-titanium instruments manufactured with different thermal treatments. *J. Endod.* **2015**, *41*, 67–71. [CrossRef]

26. Ninan, E.; Berzins, D.W. Torsion and bending properties of shape memory and superelastic nickel-titanium rotary instruments. *J. Endod.* **2013**, *39*, 101–104. [CrossRef]

27. De Arruda Santos, L.; Bahia, M.G.; de Las Casas, E.B.; Buono, V.T. Comparison of the mechanical behavior between controlled memory and superelastic nickel-titanium files via finite element analysis. *J. Endod.* **2013**, *39*, 1444–1447. [CrossRef] [PubMed]

28. Nehme, W.; Naaman, A.; Diemer, F.; Leotta, M.L.; La Rosa, G.R.M.; Pedullà, E. Influence of different heat treatments and temperatures on the cyclic fatigue resistance of endodontic instruments with the same design. *Clin. Oral Investig.* **2022**, in press. [CrossRef] [PubMed]

29. Alghamdi, S.; Huang, X.; Haapasalo, M.; Mobuchon, C.; Hieawy, A.; Hu, J.; Wang, Z.; Sobotkiewicz, T.; Shen, Y. Effect of curvature location on fatigue resistance of five nickel-titanium files determined at body temperature. *J. Endod.* **2020**, *46*, 1682–1688. [CrossRef]

30. Silva, E.; Giraldes, J.F.N.; de Lima, C.O.; Vieira, V.T.L.; Elias, C.N.; Antunes, H.S. Influence of heat treatment on torsional resistance and surface roughness of nickel-titanium instruments. *Int. Endod. J.* **2019**, *52*, 1645–1651. [CrossRef] [PubMed]

31. Oh, S.; Kum, K.Y.; Kim, H.J.; Moon, S.Y.; Kim, H.C.; Chaniotis, A.; Perinpanayagam, H.; Pedullá, E.; Chang, S.W. Bending resistance and cyclic fatigue resistance of WaveOne Gold, Reciproc Blue, and HyFlex EDM instruments. *J. Dent. Sci.* **2020**, *15*, 472–478. [CrossRef] [PubMed]

32. Martins, J.N.R.; Silva, E.; Marques, D.; Belladonna, F.G.; Simões-Carvalho, M.; da Costa, R.P.; Ginjeira, A.; Braz Fernandes, F.M.; Versiani, M.A. Comparison of five rotary systems regarding design, metallurgy, mechanical performance, and canal preparation-a multimethod research. *Clin. Oral Investig.* **2022**, *26*, 3299–3310. [CrossRef] [PubMed]

33. Uygun, A.D.; Kol, E.; Topcu, M.K.; Seckin, F.; Ersoy, I.; Tanriver, M. Variations in cyclic fatigue resistance among ProTaper Gold, ProTaper Next and ProTaper Universal instruments at different levels. *Int. Endod. J.* **2016**, *49*, 494–499. [CrossRef]

34. MicroMega, 2Shape. Available online: https://micro-mega.com/wp-content/uploads/2018/03/60301807-C_Brochure-2Shape_EN_WEB.pdf (accessed on 1 November 2022).

35. International Organization for Standardization. International Standard ISO 3630-1:2019(E): Root-Canal Instruments—Part 1: General Requirements and Test Methods. 2019. Available online: https://www.iso.org/obp/ui/#iso:std:iso:3630:-1:ed-3:v1:en (accessed on 1 September 2022).

36. Oh, S.; Jeon, B.K.; Chang, S.W. Mechanical properties and torque/force generation of XP-Endo Shaper, Trunatomy, Spring Endo File, and Spring Endo Heated Finish File, Part 1. *Appl. Sci.* **2022**, *12*, 10393. [CrossRef]

37. Lopes, H.P.; Elias, C.N.; Siqueira, J.F., Jr.; Soares, R.G.; Souza, L.C.; Oliveira, J.C.; Lopes, W.S.; Mangelli, M. Mechanical behavior of pathfinding endodontic instruments. *J. Endod.* **2012**, *38*, 1417–1421. [CrossRef]

38. Ha, J.H.; Kwak, S.W.; Versluis, A.; Kim, H.C. Buckling resistance of various nickel-titanium glide path preparationinstruments in dynamic or static mode. *J. Endod.* **2020**, *46*, 1125–1129. [CrossRef]

39. Bürklein, S.; Börjes, L.; Schäfer, E. Comparison of preparation of curved root canals with Hyflex CM and Revo-S rotary nickel-titanium instruments. *Int. Endod. J.* **2014**, *47*, 470–476. [CrossRef]

40. Marceliano-Alves, M.F.; Sousa-Neto, M.D.; Fidel, S.R.; Steier, L.; Robinson, J.P.; Pécora, J.D.; Versiani, M.A. Shaping ability of single-file reciprocating and heat-treated multifile rotary systems: A micro-CT study. *Int. Endod. J.* **2015**, *48*, 1129–1136. [CrossRef]

41. McGuigan, M.B.; Louca, C.; Duncan, H.F. Endodontic instrument fracture: Causes and prevention. *Br. Dent. J.* **2013**, *214*, 341–348. [CrossRef] [PubMed]

42. Shen, Y.; Huang, X.; Wang, Z.; Wei, X.; Haapasalo, M. Low environmental temperature influences the fatigue resistance of nickel-titanium files. *J. Endod.* **2018**, *44*, 626–629. [CrossRef]

43. Oh, S.; Kum, K.Y.; Cho, K.; Lee, S.H.; You, S.H.; Go, J.; Jeon, B.K.; Kim, S.W.; Kim, T.H.; Jang, J.H.; et al. Torsional and bending properties of V Taper 2H, ProTaper NEXT, NRT, and One Shape. *BioMed Res. Int.* **2019**, *2019*, 6368958. [CrossRef]

44. Lopes, H.P.; Gambarra-Soares, T.; Elias, C.N.; Siqueira, J.F., Jr.; Inojosa, I.F.; Lopes, W.S.; Vieira, V.T. Comparison of the mechanical properties of rotary instruments made of conventional nickel-titanium wire, M-wire, or nickel-titanium alloy in R-phase. *J. Endod.* **2013**, *39*, 516–520. [CrossRef] [PubMed]

45. Ha, J.H.; Lee, C.J.; Kwak, S.W.; El Abed, R.; Ha, D.; Kim, H.C. Geometric optimization for development of glide path preparation nickel-titanium rotary instrument. *J. Endod.* **2015**, *41*, 916–919. [CrossRef] [PubMed]

46. Alqedairi, A.; Alfawaz, H.; Abualjadayel, B.; Alanazi, M.; Alkhalifah, A.; Jamleh, A. Torsional resistance of three ProTaper rotary systems. *BMC Oral Health* **2019**, *19*, 124. [CrossRef] [PubMed]

47. Liang, Y.; Yue, L. Evolution and development: Engine-driven endodontic rotary nickel-titanium instruments. *Int. J. Oral. Sci.* **2022**, *14*, 12. [CrossRef]

48. Amine, M.; Merdma, W.; El Boussiri, K. Electrogalvanism in Oral Implantology: A Systematic Review. *Int. J. Dent.* **2022**, *2022*, 4575416. [CrossRef] [PubMed]

49. Sfondrini, M.F.; Cacciafesta, V.; Maffia, E.; Scribante, A.; Alberti, G.; Biesuz, R.; Klersy, C. Nickel release from new conven tional stainless steel, recycled, and nickel-free orthodontic brackets: An in vitro study. *Am. J. Orthod. Dentofac. Orthop.* **2010**, *137*, 809–815. [CrossRef]